Asymptotic studies of Mohr-Coulomb and Drucker-Prager soft thin layers

Frédéric Lebon, Sylvie Ronel-Idrissi

▶ **To cite this version:**

Frédéric Lebon, Sylvie Ronel-Idrissi. Asymptotic studies of Mohr-Coulomb and Drucker-Prager soft thin layers. Steel and Composite Structures, 2004, 4, pp.133-147. 10.12989/scs.2004.4.2.133 . hal-00088239

HAL Id: hal-00088239

https://hal.science/hal-00088239v1

Submitted on 30 May 2018

HAL is a multi-disciplinary open access archive for the deposit and dissemination of scientific research documents, whether they are published or not. The documents may come from teaching and research institutions in France or abroad, or from public or private research centers.

L'archive ouverte pluridisciplinaire **HAL**, est destinée au dépôt et à la diffusion de documents scientifiques de niveau recherche, publiés ou non, émanant des établissements d'enseignement et de recherche français ou étrangers, des laboratoires publics ou privés.

Asymptotic analysis of Mohr-Coulomb and Drucker-Prager soft thin layers

F. Lebon† and S. Ronel-Idrissi‡

Laboratoire Mécanique Matériaux Structures, Université Claude Bernard Lyon 1, 82 Bd Niels Bohr, Domaine Scientifique de la Doua, 69622 Villeurbanne Cedex, France

(Received July 19, 2003, Revised February 26, 2004, Accepted April 8, 2004)

Abstract. This paper deals with the asymptotic analysis of Mohr-Coulomb and Drucker-Prager soft thin layers bonded with elastic solids. In the first part, a mathematical analysis shows how to obtain an interface law that replaces mechanically and geometrically the thin layer. This law is strongly non-linear and couples microscopic and macroscopic scales. In the second part of the paper, the microscopic terms are quantified numerically, and it is shown that they can be neglected.

Key words: asymptotic studies; elasto-plasticity; non-associated laws; interface laws; finite elements.

1. Introduction

The objective of this paper is to analyse soft thin layers in order to replace them by interface laws. The aim of our work is to study non-linear soft materials; especially, we focus on the case of non-associated elastic-plastic materials of Mohr-Coulomb and Drucker-Prager kind. These materials are described in the implicit standard materials framework based on the bipotential theory (Hjiaj, de Saxcé, Mroz 2002).

During the last two decades several authors have developed asymptotic theories applied to thin layers (Suquet 1988),(Ait Moussa 1989),(Klarbring 1991),(Licht, Michaille 1996), (Lebon, Ould Khaoua, Licht 1998), (Bayada and Lhalouani 2001). The idea of this work is to replace a thin layer bonded with two substrata by an interface law which keeps in memory the mechanical and geometrical characteristics of the layer. The motivation of this analyse is the complexity of the numerical approach:

- the thickness of the layer is small regarding the substrata dimensions
- the stiffness of the layer is weak compared with the substrata rigidities.

The theory consists in considering that the geometrical and mechanical parameters of the layer tend to zero and to analyse the limit problem. In this limit problem, the layer vanishes geometrically and an interface law replaces it. Using this theory, simplified models of interface are obtained which are easier to compute by finite element software. On the one hand, this theory permits to justify empirical interface laws that one can find in the literature and on the other hand, to find new interface laws. In previous papers, different kinds of behaviour (elasticity, visco-elasticity, plasticity, ...) and kinematics

†Professor
‡Assistant Professor

(small perturbations, plates, finite deformations, ...) have been dealt with. Our contribution in this work is concerned with non-associated elastic-plastic behaviours.

The paper is organised as follows: in the second section, the mechanical problem is presented, notations are specified and the constitutive law of the thin layer is formulated in the implicit standard materials framework. The third section is devoted to the theoretical results. The mathematical background is given and the matched asymptotic expansion method is applied to the problem with a non-linear behaviour. The mathematical results are commented. In section 4, numerical examples are presented in order to validate the theory and to quantify the terms obtained in section 3. In the last section, we close by giving conclusions and perspectives.

2. The mechanical problem

2.1. Problem definition

We consider two elastic bodies perfectly bonded with a third one which is very thin. For simplicity, we work only in two dimensions. The structure is denoted Ω with boundary $\partial\Omega$ and is referred to the local frame (O, x_1, x_2). On a part of the structure Γ_1 a surface load is applied. The structure is embedded in part Γ_0.

We denote (Fig. 1):

$$\Omega^\varepsilon = \left\{x = (x_1, x_2) \in \Omega / |x_2| > \frac{\varepsilon}{2}\right\} \qquad B^\varepsilon = \left\{x = ((x_1, x_2) \in \Omega / |x_2|) < \frac{\varepsilon}{2}\right\}$$

$$\Omega^\varepsilon_\pm = \left\{x = (x_1, x_2) \in \Omega / \pm x_2 > \frac{\varepsilon}{2}\right\} \qquad S^\varepsilon_\pm = \left\{x = (x_1, x_2) \in \Omega / \pm x_2 > \frac{\varepsilon}{2}\right\}$$

$$\Omega_\pm = \{x = (x_1, x_2) \in \Omega / \pm x_2 > 0\} \qquad S = \{x = (x_1, x_2) \in \Omega / x_2 > 0\}$$

$$\Omega_0 = \Omega_+ \cup \Omega_- \qquad \varepsilon\text{: thin layer thickness}$$

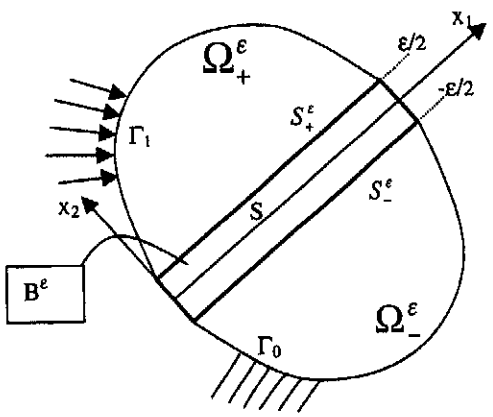

Fig. 1 Geometry of the problem

We consider the following hypotheses:

Plane problems Small strains, $e_{ij}(\boldsymbol{u}^\varepsilon) = \frac{1}{2}\left(\frac{\partial u_i^\varepsilon}{\partial x_j} + \frac{\partial u_j^\varepsilon}{\partial x_i}\right)$ Additive decomposition of strains: $\boldsymbol{e}(\boldsymbol{u}^\varepsilon)=\boldsymbol{e}^e(\boldsymbol{u}^\varepsilon)+\boldsymbol{e}^p(\boldsymbol{u}^\varepsilon)$, respectively elastic strain and plastic strain.	Ω^ε are deformable bodies $S_\pm^\varepsilon$ is the interface between the adhesive and the adherent B^ε is the thin layer S is the surface to which the adhesive tends geometrically

The two bodies $\Omega_\pm^\varepsilon$ (adherent) are supposed to be elastic and the joint B^ε (adhesive) to be elastic-plastic. In the next section, details of the behaviour of the thin layer are given.

Denoting by a_{ijkl} the elasticity parameters, we have to solve the following problem:

Find $(\boldsymbol{u}^\varepsilon, \boldsymbol{\sigma}^\varepsilon)$ such as:

$\sigma_{ij,j}^\varepsilon = 0 \quad \text{in}\Omega_0$ $\sigma_{ij}^\varepsilon = a_{ijkl}\ e_{kl}(\boldsymbol{u}^\varepsilon)\ \text{in}\Omega^\varepsilon$ + behaviour law in B^ε	$\boldsymbol{u}^\varepsilon = 0$ on Γ_0 $\boldsymbol{\sigma}^\varepsilon \boldsymbol{n} = \boldsymbol{F}$ on Γ_1 $\left\|\boldsymbol{u}^\varepsilon\right\|_{s_\pm^\varepsilon} = \boldsymbol{0}$ and $\left\|\boldsymbol{\sigma}^\varepsilon n\right\|_{s_\pm^\varepsilon} = \boldsymbol{0}$ (1)

$[\,]_{s_\pm^\varepsilon}$ is the jump on the boundary $S_\pm^\varepsilon$ and $\boldsymbol{n}$ is the external normal unit.

2.2. Behaviour in the thin layer

In this section, we describe the behaviour of the material in the thin layer. We consider that it obeys a non-associated elastic-plastic law. This kind of material is not in the family of generalized standard materials (Nguyen 1973) but in the class of implicit standard materials described in terms of the bi-potential theory (Hjiaj, de Saxcé, Mroz 2002). In the case of generalized standard materials, we need to define a potential and a pseudo-potential of dissipation. In the framework of implicit standard materials, the behaviour is described introducing a bi-potential b and a bi-potential b_p which depend on two tensorial fields, the stress tensor $\boldsymbol{\sigma}$ and the elastic strain tensor $\boldsymbol{e}^e$ (resp. the plastic-strain rate tensor $\dot{\boldsymbol{e}}^p$). The behaviour law is built from the derivation of these two bi-potentials:

$$\boldsymbol{\sigma} = \frac{\partial b}{\partial \boldsymbol{e}^e}, \quad \boldsymbol{e}^e = \frac{\partial b}{\partial \boldsymbol{\sigma}} \tag{2}$$

$$\boldsymbol{\sigma} = \frac{\partial b_p}{\partial \dot{\boldsymbol{e}}^p}, \quad \dot{\boldsymbol{e}}^p = \frac{\partial b_p}{\partial \boldsymbol{\sigma}} \tag{3}$$

In the case of a Drucker-Prager material, the bi-potential of dissipation is written:

$$b_p(\boldsymbol{\sigma}, \dot{\boldsymbol{e}}^p) = c\dot{e}_m^p + (tg\,\theta - tg\,\varphi)(s_m - c)\left\|\dot{\boldsymbol{e}}^p\right\| + \chi_{K_e}(\dot{\boldsymbol{e}}^p) + \chi_{K\sigma}(\boldsymbol{\sigma}) \tag{4}$$

where χ_A is the indicator function of set A:

$$\chi_A(x) = 0, \text{ if } x \in A,\ \chi_A(x) = +\infty \text{ otherwise}$$

Sets $\boldsymbol{K}_\sigma$ and $\boldsymbol{K}_e$ are defined by:

$$\boldsymbol{K}_\sigma = \{\boldsymbol{\sigma}, \|s\| \leq c - tg\varphi\, s_m\} \tag{5}$$

$$\boldsymbol{K}_e = \{\dot{\boldsymbol{e}}^p, \dot{e}^p_m \geq tg\theta \|\dot{\boldsymbol{e}}^p_d\|\} \tag{6}$$

$$s_m = \frac{1}{3} tr(\boldsymbol{\sigma}), \text{ (hydrostatic pressure)} \tag{7}$$

$$s = \boldsymbol{\sigma} - s_m \boldsymbol{Id}, \text{ (stress deviator tensor)} \tag{8}$$

$$\dot{e}^p_m = \frac{1}{3} tr(\dot{\boldsymbol{e}}^p) \tag{9}$$

$$\dot{\boldsymbol{e}}^p_d = \dot{\boldsymbol{e}}^p - \dot{e}^p_m \boldsymbol{Id} \tag{10}$$

$$\|a\| = \sqrt{\frac{3}{2} a_{ij} a_{ij}} \text{ for any tensor } a \text{ (Von Mises norm)}$$

c is the cohesion, φ is the friction angle and θ is the dilatance angle.

In the case of a Mohr-Coulomb material, the bi-potential of dissipation is written:

$$b_p(\boldsymbol{\sigma}, \dot{\boldsymbol{e}}^p) = c\dot{e}^p_m - tg\varphi(n_\sigma - c)\|\dot{\boldsymbol{e}}^p\| + \chi_{K_e}(\dot{\boldsymbol{e}}^p) + \chi_{K\sigma}(\boldsymbol{\sigma}) \tag{11}$$

Sets $\boldsymbol{K}_\sigma$ and $\boldsymbol{K}_e$ are defined by:

$$\boldsymbol{K}_\sigma = \{\boldsymbol{\sigma}, \|t_\sigma\| \leq c - tg\varphi n_\sigma\} \tag{12}$$

$$\boldsymbol{K}_e = \{\dot{\boldsymbol{e}}^p, \dot{e}^p_m \geq 0\} \tag{13}$$

where t_σ and n_σ are respectively the shear and normal stresses associated to the stress tensor $\boldsymbol{\sigma}$. In the following, the material will be supposed isotropic.

3. Theoretical results

3.1. Mathematical background

The idea of matched asymptotic expansions (Eckhaus 1979) is to find two expansions of the displacement $\boldsymbol{u}^\varepsilon$ and the stress σ^ε in the powers of ε, that is, an external one in the bodies and an internal in the joint, and to connect these two expansions in order to obtain the same limit. We will obtain relations in the internal expansions that we will express from values that intervene in the external expansions.

3.1.1. External expansions

The external expansion is a classical expansion in powers of ε:

$$u^\varepsilon(x_1, x_2) = u^0(x_1, x_2) + \varepsilon\, u^1(x_1, x_2) + \ldots, \tag{14}$$

$$e^m_{ij} = \frac{1}{2}\left(\frac{\partial u^m_i}{\partial x_j} + \frac{\partial u^m_j}{\partial x_i}\right) \tag{15}$$

$$e_{ij}^{\varepsilon}(\boldsymbol{u}^{\varepsilon})(x_1, x_2) = e_{ij}^{0} + \varepsilon\, e_{ij}^{1} + \ldots, \tag{16}$$

$$\sigma_{ij}^{\varepsilon}(x_1, x_2) = \sigma_{ij}^{0} + \varepsilon\, \sigma_{ij}^{1} + \ldots, \tag{17}$$

3.1.2. Internal expansions

In the internal expansion, we proceed to a blow-up of the second variable. Let $y_2 = x_2/\varepsilon$. The internal expansion gives:

$$\boldsymbol{u}^{\varepsilon}(x_1, x_2) = \boldsymbol{v}^{0}(x_1, y_2) + \varepsilon\, \boldsymbol{v}^{1}(x_1, y_2) + \ldots, \tag{18}$$

$$e_{11}^{m} = \frac{\partial v_1^m}{\partial x_1}, \quad e_{22}^{m} = \frac{\partial v_2^{m+1}}{\partial y_2}, \quad e_{12}^{m} = \frac{1}{2}\left(\frac{\partial v_2^m}{\partial x_1} + \frac{\partial v_1^{m+1}}{\partial y_2}\right), \tag{19}$$

$$e_{ij}^{\varepsilon}(\boldsymbol{u}^{\varepsilon})(x_1, y_2) = \varepsilon^{-1} e_{ij}^{-1} + e_{ij}^{0} + \varepsilon e_{ij}^{1} + \ldots, \tag{20}$$

$$\sigma_{ij}^{\varepsilon}(x_1, y_2) = \varepsilon^{-1}\tau_{ij}^{-1} + \tau_{ij}^{0} + \varepsilon\tau_{ij}^{1} + \ldots, \tag{21}$$

We use the convention

$$v^m = 0,\ m < 0,\ \tau^m = 0,\ m < -1 \tag{22}$$

where m is the expansion order.

3.1.3. Continuity conditions

The third step of the method consists of the connection of the two expansions. We choose some intermediate points defined by $x_2 = \pm\, \zeta\, \varepsilon^t$, $0 < t < 1$, $\zeta \in\ ]0,+\infty[$. When ε tends to zero, x_2 tends to $0^{\pm}$ and $y_2 = x_2/\varepsilon$ tends to $\pm\infty$. The principle of the method consists in assuming that the two expansions give the same asymptotic limits, that is:

(i) $v^0(x_1, \pm\infty) = u^0(x_1, 0^{\pm})$, (23)
(ii) $\tau^{-1}(x_1, \pm\infty) = 0$, (24)
(iii) $\tau^0(x_1, \pm\infty) = \sigma^0(x_1, 0^{\pm})$. (25)

3.2. Mathematical results

3.2.1. Equilibrium equations at order 2

We develop the equation div $\sigma = 0$. In this paragraph, we consider the equilibrium equations at order -2; we obtain:

$$\frac{\partial \tau_{i2}^{-1}}{\partial y_2} = 0 \tag{26}$$

Thus, we get

$$\tau_{i2}^{-1}(x_1, y_2) = \tau_{i2}^{-1}(x_1, \pm\infty) = 0 \tag{27}$$

The elasticity law in the bodies gives:

$$\tau_{i2}^{-1}(x_1, y_2) = a_{12j2}\frac{\partial v_j^0}{\partial y_2}, \quad \tau_{11}^{-1}(x_1, y_2) = a_{11j1}\frac{\partial v_j^0}{\partial y_2} \tag{28}$$

Thus, we have

$$\frac{\partial v_j^0}{\partial y_2} = 0 \text{ and } v^0(x_1, y_2) = v^0(x_1), |y_2| > 1/2 \tag{29}$$

We have $\tau_{i2}^{-1} = 0$ in the bodies and, due to the matched conditions $v^0(x_1, \pm|y_2|)=u^0(x_1, 0^{\pm})$.

3.2.2. Equilibrium equations at order 1

We have

$$\frac{\partial \tau_{i2}^0}{\partial y_2} = 0 \tag{30}$$

The connection conditions give

$$\tau_{i2}^0(x_1, \pm|y_2|) = \sigma_{i2}^0(x_1, 0^{\pm}) \tag{31}$$

with $y_2 = x_2/\varepsilon$ tends to $\pm\infty$ when ε tends to zero.

3.2.3. Elasticity of the thin layer

The asymptotic expansions give:

$$\varepsilon^{-1} + \tau_{ij}^{-1} + \tau_{ij}^0 + \varepsilon\tau_{ij}^1 + \ldots = \lambda(\varepsilon^{-1}(e_{kk}^{-1})^e + (e_{kk}^0)^e + \ldots)\delta_{ij} + \mu(\varepsilon^{-1}(e_{ij}^{-1})^e + (e_{ij}^0)^e + \ldots) \tag{32}$$

where $(e_{ij}^l)^e$ is the elastic part of e_{ij}^l.

Note that before the beginning of plastification, the plastic strain is equal to zero, so the strain is reduced to the elastic strain.

We have supposed that the layer is thin and soft, that is, the thickness is small ($\varepsilon\to 0$) and the stiffness coefficients are small ($\lambda\to 0$, $\mu\to 0$). As we can see in the expansions, the identification of the different orders depends on the relative behaviour of the Lamé coefficients λ and μ with respect to the thickness ε. In fact the limit contact law depends on the two ratios λ/ε and μ/ε. We have nine possible relative variations of these two ratios corresponding to the behaviour of the coefficients (zero, a positive value, infinity). In the following, we note $\bar{f} = \lim_{\varepsilon\to 0} f/\varepsilon$. In particular, we denote by $\bar{\lambda} = \lim_{\varepsilon\to 0} \lambda/\varepsilon$ and $\bar{\mu} = \lim_{\varepsilon\to 0} \mu/\varepsilon$ the limits associated to Lamé coefficients. In the following, only one case is presented, that is the more representative case where the limits are positive values. All the other cases can be deduced easily.

Before the beginning of plastification, the identification of the terms of order zero gives:

$$\tau_{12}^0(x_1) = \bar{\mu}\frac{\partial v_1^0}{\partial y_2} \tag{33}$$

$$\tau_{22}^0(x_1) = (\bar{\lambda} + 2\bar{\mu})\frac{\partial v_2^0}{\partial y_2} \tag{34}$$

By integration of Eq. (33), Eq. (34) and using the connection conditions Eq. (23), Eq. (25), we find the elasto-static case which is now classical (Ait-Moussa 1989):

$$\sigma \boldsymbol{n} = \boldsymbol{K}_L\,[\boldsymbol{u}] \tag{35}$$

Matrix $\boldsymbol{K}_L$ is diagonal and its diagonal terms are equal to $\bar{\mu}$ and $\bar{\lambda} + 2\bar{\mu}$ respectively. [] is the jump on boundary S.

3.2.4. Elasto-plasticity

The most interesting case is when the plastic threshold is reached.

For a Mohr-Coulomb material this threshold

$$\left|\varepsilon^{-1}\boldsymbol{t}_\tau^{-1}\boldsymbol{t}_\tau^0+\ldots\right| \le c - tg\,\varphi(\varepsilon^{-1}n_\tau^{-1} + n_\tau^0+\ldots) \tag{36}$$

is replaced by

$$\left|t_\tau^0\right| \le c - tg\,\varphi(n_\tau^0) \tag{37}$$

where $\boldsymbol{t}_\tau^l$ is the shear stress part of $\boldsymbol{\tau}^1$ and n_τ^l is the normal stress associated to $\boldsymbol{\tau}^1$.

For a Drucker-Prager material this threshold

$$\left\|\varepsilon^{-1}\boldsymbol{s}_\tau^{-1} + \boldsymbol{s}_\tau^0+\ldots\right\| \le c - tg\,\varphi(\varepsilon^{-1}s_{\tau m}^{-1} + s_{\tau m}^0+\ldots) \tag{38}$$

is replaced by

$$\left\|\boldsymbol{s}_\tau^0\right\| \le c - tg\,\varphi(s_{\tau m}^0) \tag{39}$$

where $\boldsymbol{s}_\tau^l$ is the deviatoric part of $\boldsymbol{\tau}^1$ and $s_{\tau m}^l$ is the pressure associated to $\boldsymbol{\tau}^1$.

We obtain from Eq. (32)

$$\tau_{12}^0(x_1) = 2\bar{\mu}\left(\frac{1}{2}\frac{\partial v_1^0}{\partial y_2} - (e_{12}^{-1})^p\right) \tag{40}$$

$$\tau_{22}^0(x_1) = \bar{\lambda}\left(\frac{\partial v_2^0}{\partial y_2} - (e_{11}^{-1})^p - (e_{22}^{-1})^p\right) - 2\bar{\mu}\left(\frac{\partial v_2^0}{\partial y_2} + (e_{22}^{-1})^p\right) \tag{41}$$

where $(e_{ij}^{-1})^p$ is the plastic part of e_{ij}^{-1}. Using a notation similar to Eq. (35), we denote by

$$[u_1^p] = 2\int_{-1/2}^{1/2} (e_{12}^{-1})^p\,dy_2 \tag{42}$$

and

$$[u_2^p] = \frac{1}{\bar{\lambda} + 2\bar{\mu}} \int_{-1/2}^{1/2} (\bar{\lambda}(e_{11}^{-1})^p + (\bar{\lambda} + 2\bar{\mu})(e_{22}^{-1})^p)\,dy_2 \tag{43}$$

Considering that the elastic part $(e_{11}^{-1})^e$ is equal to zero, it seems convenient to suppose that $(e_{11}^{-1})^p$ is equal to zero too (that is the deformation e_{11}^{-1} is small), and thus

$$[u_2^p] = \int_{-1/2}^{1/2} (e_{22}^{-1})^p dy_2 \tag{44}$$

Note that this hypothesis is confirmed numerically.

So, we obtain from Eq. (32)

$$\sigma_{12} = \bar{\mu}([u_1^e] - [u_1^p]) \tag{45}$$

$$\sigma_{22} = (\bar{\lambda} + 2\bar{\mu})([u_2^e] - [u_2^p]) \tag{46}$$

and integrating Eq. (3)

- Drucker-Prager condition: $[\dot{\boldsymbol{u}}^p] = -k_{DP}\boldsymbol{s}\boldsymbol{n}, k_{DP} > 0$ (47)
- Mohr-Coulomb condition: $[\dot{\boldsymbol{u}}^p] = -k_{MC}\bar{\boldsymbol{t}}, k_{MC} > 0$ (48)

Vector $\bar{t}$ corresponds to the direction of the shear stress.

The limit problem is quite different in this non-linear case. The plastic yield and the plastic law depend on a local problem. Local problem means that they do not depend on the stress vector but on all the components of the stress tensor in the thin layer (Eq. (47), Eq. (48)). On the one hand the thin layer vanishes from a geometrical point of view ($\varepsilon \to 0$) and on the other hand, in the limit problem, we have a strong coupling between the interface law (Eq. (45), Eq. (46)) and a problem in the thin layer because the local stress tensor is a priori unknown in Eq. (47), Eq. (48).

3.2.5. Local problem

In order to determine the threshold and the direction of sliding, we have to solve the following elastic-plastic problem (here Drucker-Prager model, results obtained for Mohr-Coulomb model are of the same kind) in the rectangle domain $S \times [-1/2,1/2]$:

$$\begin{cases} \dfrac{\partial \sigma_{i2}}{\partial y_2} = 0 \\ \boldsymbol{e} = \boldsymbol{e}^e + \boldsymbol{e}^p \\ \sigma_{ij} = \lambda(e_{kk})^e \delta_{ij} + 2\mu(e_{ij})^e \\ \|\boldsymbol{s}\| \le c - tg\varphi s_m \\ \text{If } \|\boldsymbol{s}\| < c - tg\varphi s_m \text{ then } \dot{\boldsymbol{e}}^p = 0 \\ \text{If } \|\boldsymbol{s}\| = c - tg\varphi s_m \text{ then } \dot{\boldsymbol{e}}^p = -k\boldsymbol{s} \end{cases} \tag{49}$$

Due to the fact that the solution does not depend on the thickness, we have to solve only a "one-dimensional problem". We observe that we obtain a "pseudo-penalized-Coulomb" law of friction. Note that if the direction of flow is equal to (or approximated by) x_1, we find the classical Coulomb law of friction.

4. Numerical results

4.1. Geometry of the examples

In this section, we present three numerical tests. The first one is a long square bar bonded with a rigid obstacle. The width of the bar is equal to 100 mm and the thickness of the thin layer is equal to 1 mm. A load is applied on the left part of the structure. The second example is the same bar with a load applied both on the left part and on the top of the structure. The load on the top is twice smaller than the load on the left part. These examples are treated considering that the thin layer obeys Drucker-Prager behaviour. Details on the mechanical characteristics are given in Fig. 2.

The third example is a dovetail assembly. Due to the symmetry of the problem, only a half of the structure is considered. A thin layer is bonded between the two elastic parts of the assembly. The layer is oblique with regards to the loads. The loads are applied at the bottom of the structure. The dimensions and

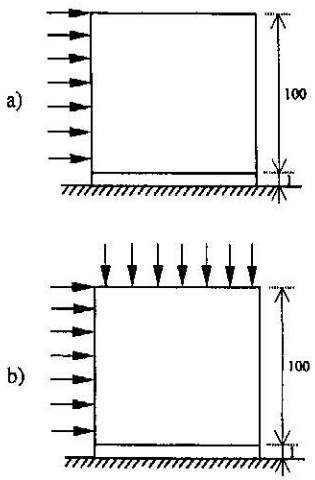

Thickness (mm)	1
Substrata Young modulus (Gpa)	200
Substrata Poisson ratio	0.3
Thin layer Young modulus (Gpa)	30
Thin layer Poisson ratio	0.3
Cohesion (Mpa)	1
Friction angle (°)	30
Dilatance angle (°)	0
F_1 (N/mm)	a) $(3.6E^{-2})$*step b) $(3.6E^{-2})$*step
F_2 (N/mm)	a) 0 b) $(1.8E^{-2})$*step
Finite element	8-node quadrangle

Fig. 2 The first two examples: a bar bonded with a plane (the dimensions are in mm)

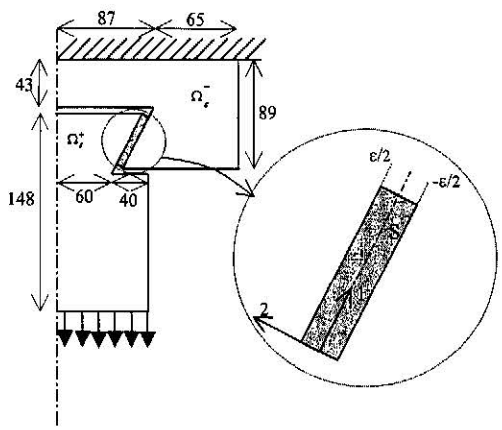

Thickness (mm)	0.5
Substrata Young modulus (Gpa)	240
Substrata Poisson ratio	0.38
Thin layer Young modulus (Gpa)	30
Thin layer Poisson ratio	0.3
Cohesion (Mpa)	1
Friction angle (°)	30
Dilatance angle (°)	0
F_1 (N/mm)	$(0.8E^{-2})$*step
Finite element	6-node triangle

Fig. 3 The third example: a dovetail assembly (the dimensions are in mm)

the mechanical characteristics are given in Fig. 3. As for the previous examples, the material in the thin layer obeys Drucker-Prager elasto-plasticity.

The set of these three examples is quite general and representative of the mechanical phenomena induced by non-linearities and the small characteristics of the thin layer. In the following section, numerical results obtained using these three examples are presented and commented.

4.2. Numerical synthesis

4.2.1. Elastic domain

The computations are done using ANSYS software (ANSYS 2002). In the first part of the numerical synthesis, we observe the results in the elastic domain (Fig. 4). Fig. 4(a) corresponds to example 1 at step 13, Fig. 4(b) corresponds to example 2 at step 15 and Fig. 4(c) to example 3 at step 30. In these figures, we represent the tangential stress/tangential displacement ratio. As expected from the theory, this ratio is close to μ/ε, where μ is the second Lamé coefficient, $\mu = E/2(1+\nu)$ (Eq. (35)). We observe that examples 1 and 2 give the same value because the thin layers have the same mechanical characteristics. A similar result is obtained for the normal components. In this case the limit is equal to $(l + 2\mu)/\varepsilon$, with $\lambda = E\nu/(1-\nu^2)$. These results establish the validity of our theory in the elastic case; note that due to boundary effects, this theory is not valid at the extremities.

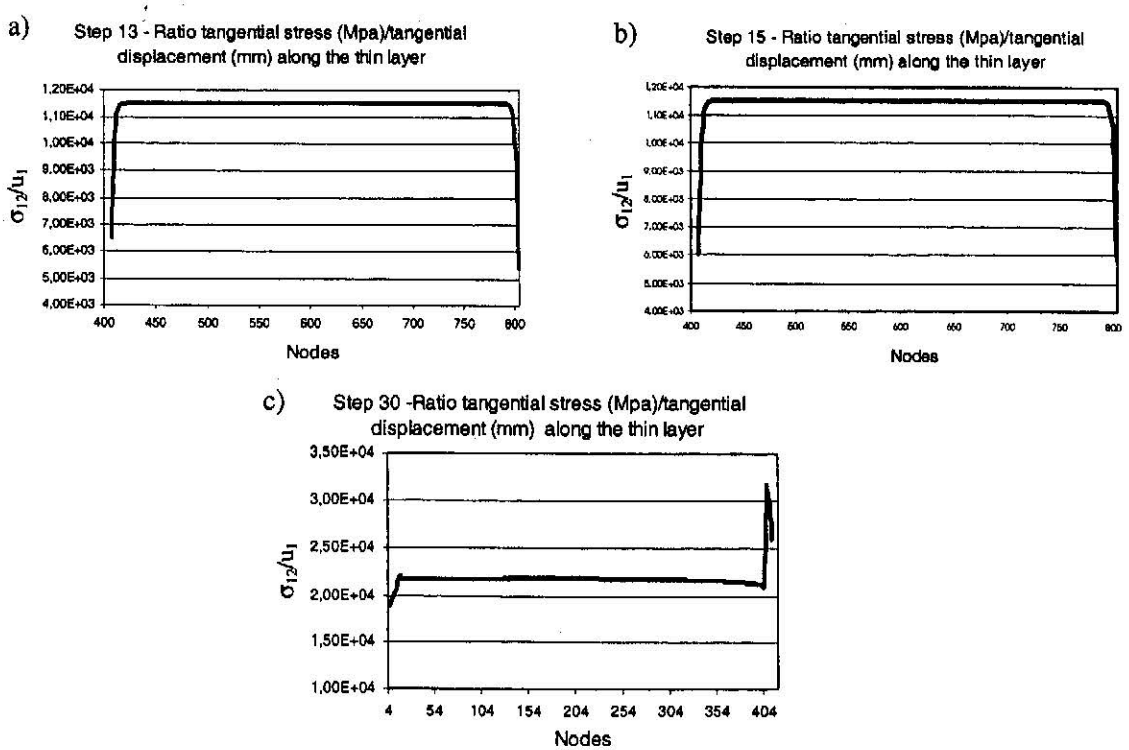

Fig. 4 Tangential stress (MPa)/tangential displacement (mm) ratio in the elastic domain along the interface substratum/thin layer a) example 1 at step 13 b) example 2 at step 15 c) example 3 at step 30

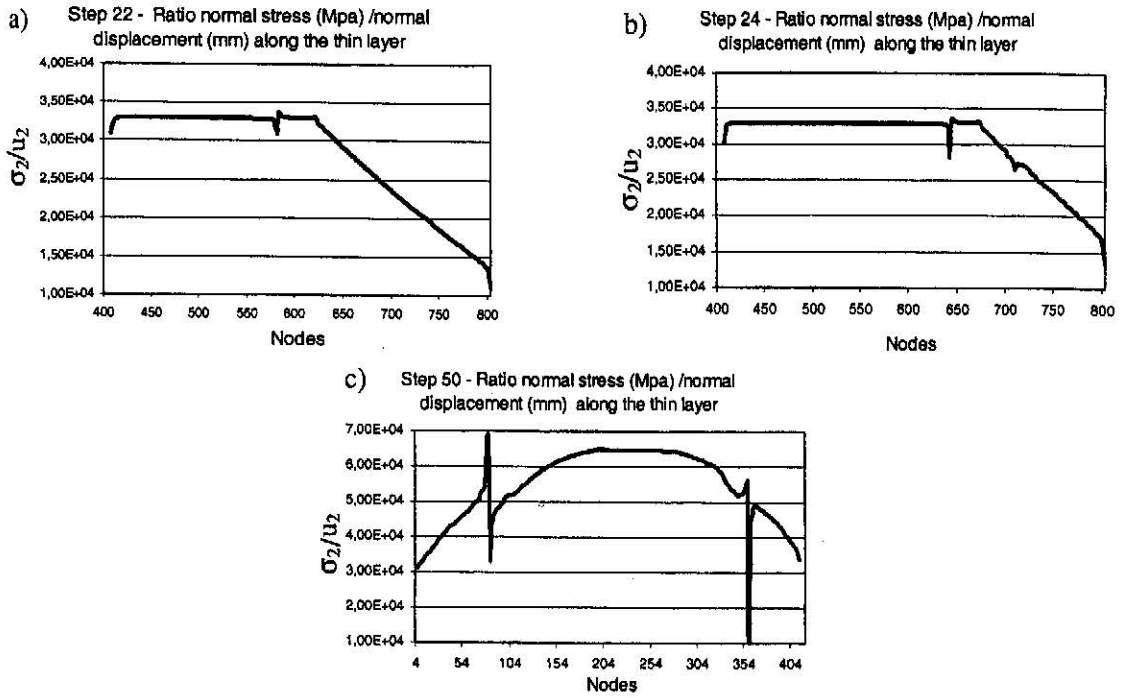

Fig. 5 Normal stress (MPa) /normal displacement (mm) ratio in the elastic-plastic domain along the interface substratum/thin layer a) example 1 at step 22 b) example 2 at step 24 c) example 3 at step 50

4.2.2. Elastic-plastic domain

We consider now the elastic-plastic domain (Fig. 5). In the elastic part, we find the previous results again. The first two examples give a stiffness density of 33000 N/mm^3 and the last example gives 64800 N/ mm^3, these values correspond to $(\lambda+2\mu)/\varepsilon$ (Eq. (35)). In the plastic zones (Eq. (39)), we do not find a constant value. In the next sections, we analyse more precisely these zones. Note in the third example that the points of discontinuity correspond to a normal displacement and a normal stress close to zero together: the thin layer is not crushing or pulling out on these nodes.

4.2.3. Plastic yield

We have shown in the theoretical part, that in the limit problem it is necessary to solve a local problem coupled with the global one. In the local problem (Eq. (49)), there are two significant quantities, which intervene: the plastic yield and the plastic flow. The aim of this section is to quantify the level of each term in the plastic yield. In fact, we want to analyse if it is possible to replace the "real" plastic yield in which all the terms of the stress tensor are considered, by a "simplified" one in which only the terms of the stress vector on the surface are taken into account.

The real plastic yield is defined by:

$$||s|| \leq c - tg\varphi\, s_m \tag{50}$$

The simplified plastic yield is defined by:

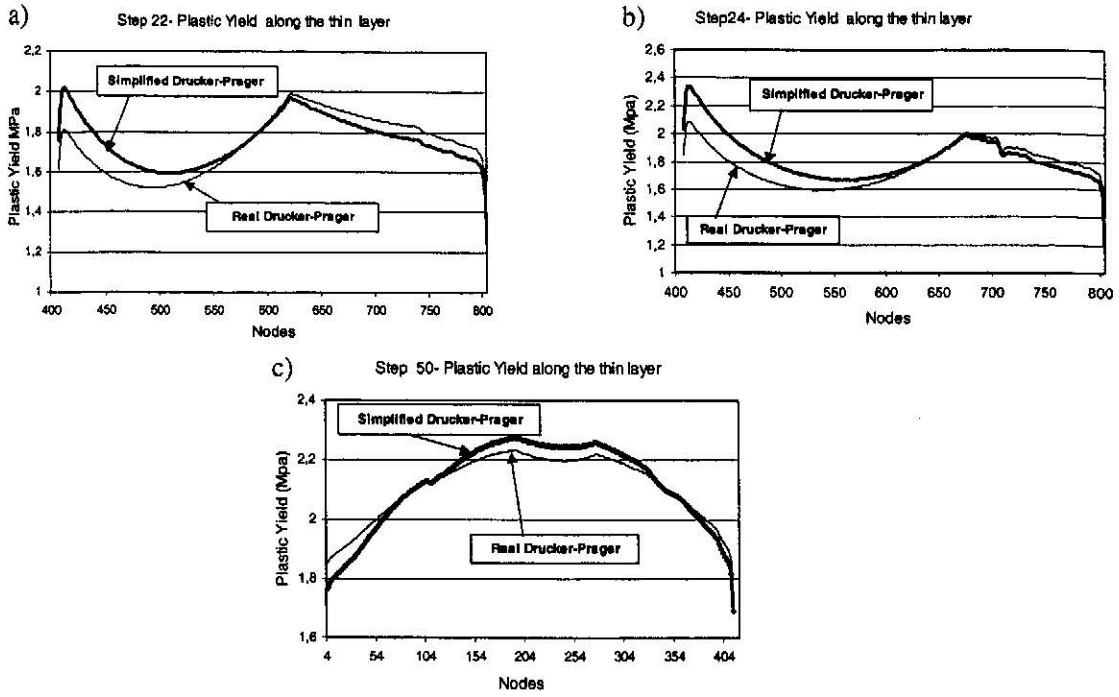

Fig. 6 Plastic yields along the substratum/thin layer interface a) example 1 at step 22 b) example 2 at step 24 c) example 3 at step 50

$$\|s_{(simp)}\| \leq c - tg\varphi \; s_{m(simp)} \tag{51}$$

We compare the real plastic yield with the simplified one which use only the terms corresponding to the stress vector. In the last formula (Eq. (51)), the stress tensor is replaced by $\sigma n \otimes_s n$, where $\otimes_s$ is the symmetrical tensorial product (s_{simp} is the deviatoric part of (σn): $s(\sigma n)$ and $s_{m(simp)}=tr(s_{simp})$). Fig. 6 shows the differences between the two plastic yields for the three examples (only the right hand side of Eq. (50) and Eq. (51) are represented). We observe a very low difference for the three examples and that this difference does not modify the initiation of the plastification. The gap is maximum in the elastic zone but generally remains lower than 5%. In the plastic zones, this gap decreases to 4% for the first two examples and to 2% for the last one. Fig. 7 shows the relative difference of the two yields for example 3 along the surface of the thin layer at step 50. As a conclusion of this study, we have shown that our simplification is valid and that it is possible to work only with the stress vector for the computation of the plastic yield.

4.2.4. Plastic strain

The aim of this section is to quantify the level of each component of the plastic strain (Eq. (3), Eq. (47), Eq. (48)). Fig. 8 shows for the three examples that the components of the plastic strain vector that is e_{12}^p and e_{22}^p are preponderant. e_{11}^p is very small compared to the two other components of the tensor (Eq. (43), Eq. (44)). As an example, in the case of the dovetail assembly, for the node 16 (at the beginning of the interface) at step 50, $e_{12}^p = -3.64\times10^{-4}$, $e_{22}^p = 8.09\times10^{-5}$ and $e_{11}= -2.92\times10^{-6}$. e_{11}^p is less than 1% of the value of e_{12}^p and close to 4% of e_{22}^p and thus can be neglected. We show in Fig. 9 the

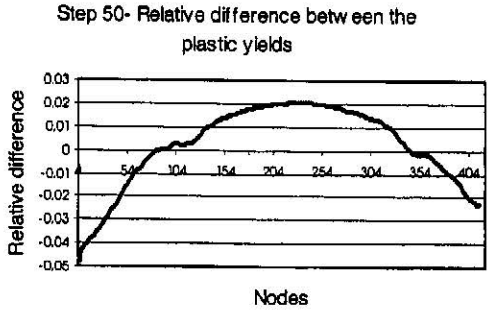

Fig. 7 Relative difference (referred to the real plastic yield) between the plastic yields (real and simplified) along the substratum/thin layer interface (example 3 at step 50)

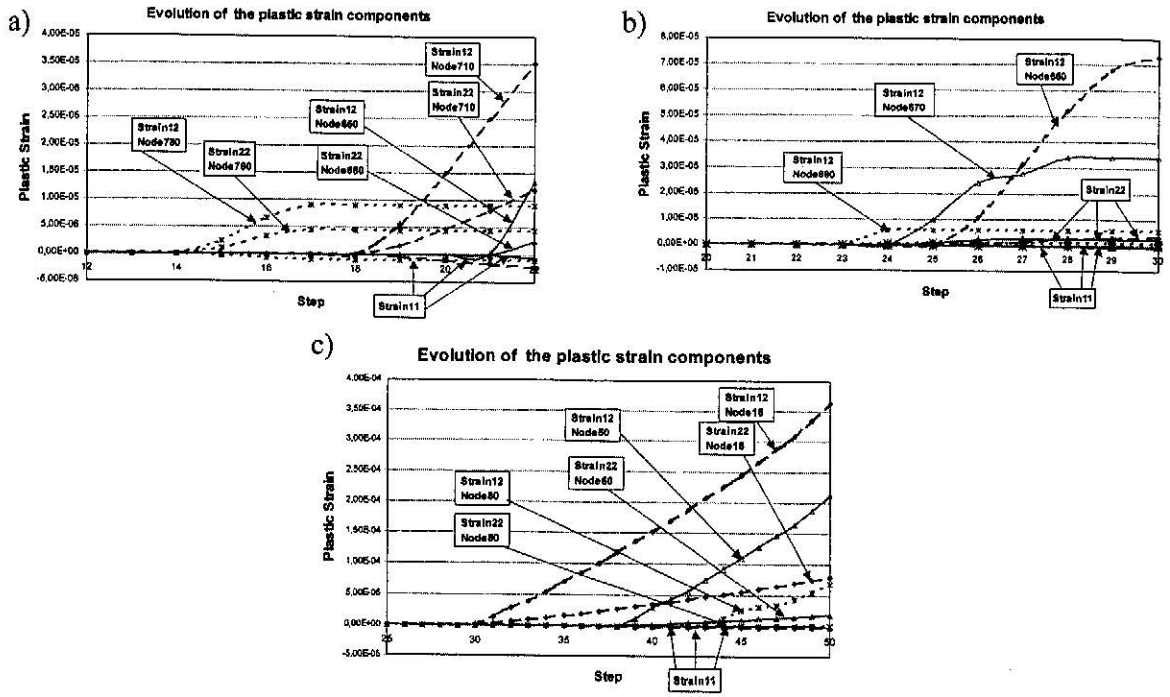

Fig. 8 Evolution of the plastic strain components for various nodes of substratum/thin layer interface: a) example 1, b) example 2, c) example 3

differences of the Von Mises norm of the "real" plastic strain and the "simplified" one. In the simplified version the plastic strain tensor e^p is replaced by $e^p \boldsymbol{n} \otimes_s \boldsymbol{n}$. The gap for the third example is close to 1%.

4.3. Conclusion of the numerical synthesis

As a conclusion, the numerical results obtained in this paper show that the local problem introduced in the theoretical study can be neglected, that is to say that the interface law can be written only in terms of stress vector. We obtain a compliance law (regularized Coulomb law), well known in the literature (Fig. 10).

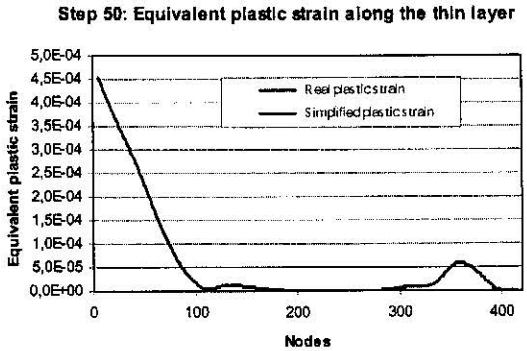

Fig. 9 Equivalent plastic strain along the substratum/thin layer interface: example 3 at step 50

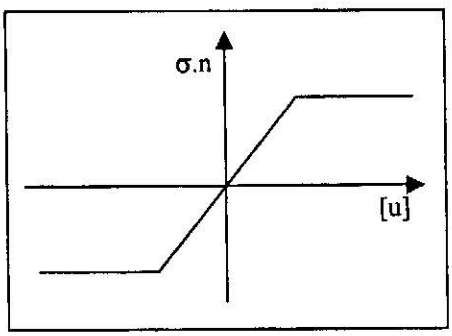

Fig. 10 The limit law: compliance law of contact

5. Conclusions

In this paper, we have analysed theoretically and numerically the asymptotic behaviour of a soft thin layer obeying to a non-associated elastic-plastic law (Drucker-Prager or Mohr-Coulomb) bonded with elastic solids; the results obtained by these two models are of the same kind. Theoretically, we have shown that when the mechanical and geometrical characteristics of the layer tend to zero, an interface law is obtained. This law couples a local problem with a global one. The numerical study has permitted to quantify the influence of the local problem and has shown that this local problem can be neglected. A classical law of compliance has been obtained. Numerical results obtained are representative of all non-associated elastic-plastic models.

A perspective of this work is to introduce damage and cracks in the thin layer in order to obtain laws which take into account the rupture between the layer and the substrata. These laws can be used to model the gluing of mechanical structures, the fibber/matrix interface in composites, the mortar/brick interface for masonries or the composite/structure interface in reinforcement techniques. Another important point is the implementation of these laws in a finite element computational software.

References

Ansys 6.1 (2002), "Documentation" Copyright © 1971, 1978, 1982, 1985, 1987, 1989, 1992-2002 by SAS IP as

an unpublished work.
Ait-Moussa, A. (1989), "Modélisation et étude des singularités d'un joint collé", Thesis, Université Montpellier II.
Bayada, G. and Lhalouani, K. (2001), "Asymptotic and numerical analysis for unilateral contact problem with Coulomb's friction between an elastic body and a thin elastic soft layer", *Asymptotic Analysis*, **25**, 329-362.
Eckhaus, W. (1979), *Asymptotic Analysis of Singular Perturbations*, North-Holland, Amsterdam.
Hjiaj, M., De Saxcé, G. and Mroz, Z. (2002), "A variational inegality-base formulation of the frictional law with non-associated sliding rule", *European Journal Mechanics A/Solids*, **21**, 49-59.
Klarbring, A. (1991), "Derivation of the adhesively bonded joints by the asymptotic expansion method", *Int. J. Eng. Science*, **29**, 493-512.
Lebon, F., Ould Khaoua, A. and Licht C. (1998), "Numerical study of soft adhesively bonded joints in finite elasticity", *Computational Mechanics*, **21**, 134-140.
Licht, C. and Michaille, G. (1997), "A modelling of elastic adhesive bonded joints", *Advances in Mathematical Sciences and Applications*, **7**, 711-740.
Nguyen,Q.S. (1973), "Matériaux élasto-visco-plastique et élastoplastique à potentiel généralisé", *Comptes Rendus de lAcadémie des Sciences*, **277**, 915-918.
Suquet, P. (1988), "Discontinuities and plasticity", *Nonsmooth Mechanics and Applications*, J.J. Moreau and P.D. Panagiotopoulos Eds., CISM Courses and Lectures, Springer-Verlag, **302**, 279-340.

CC